TURBULENT TRANSPORT IN PASSIVELY HEATED HOMOGENEOUS AND INHOMOGENEOUS FLOWS

K.R. Sreenivasan
Applied Mechanics, Mason Laboratory, Yale University, New Haven, CT 06520

S. Tavoularis
Mechanical Engineering Dept., University of Ottawa, Canada K1N 6N5

and

S. Corrsin
Chemical Engineering Dept., Johns Hopkins University, Baltimore, MD 21218

ABSTRACT

Heat flux measurements in several specially designed turbulent flows with inhomogeneous temperature field are presented and analyzed with the purpose of evaluating the performance of the gradient transport models (GTM) as well as several of the generalizations. One of the flows considered is a uniform grid-generated flow; two others are shear flows with transverse homogeneity and a constant mean velocity gradient. The fourth is the wake of a circular cylinder in which an asymmetric temperature field is created by heating a combination of thin wires located off-axis. A GTM with a constant turbulent diffusivity adequately describes the turbulent heat flux in all three homogeneous flows, while in the inhomogeneous flow, forcing gradient transport to the measured heat flux results in negative diffusivity over a part of the flow. Direct evaluation from the present and other measurements shows that none of the generalizations of the GTM is adequate. It is suggested that the large eddy transport in inhomogeneous shear flows is the possible cause for the failure of the GTMS, and that its apparent success in symmetrically heated free shear flows is largely due to the imposed boundary conditions.

NOMENCLATURE

d = diameter of the cylinder
D = turbulent diffusivity
h = height of the wind-tunnel test section
ℓ_θ = half the distance between half-maximum θ' points
L_f = longitudinal integral length scale
L_g = transverse integral length scale
L_θ = half the distance between $T_{max}/2$ points
M = mesh size of the grid
q' = $(\overline{u_i u_i})^{1/2}$
T = mean temperature rise above the ambient
u_i = velocity fluctuation in the direction i
U_i = mean velocity in the direction i
V_c = characteristic bulk convection velocity
w = wake defect velocity
x_i = coordinate axes; i=1 is along the flow and i=2 is along the direction of maximum shear.
θ = temperature fluctuation

Suffixes

o = centerline value
max = maximum value
' = root-mean-square value

INTRODUCTION

Virtually all the "classical turbulent theories" model turbulent transport of momentum, heat or a passive contaminant by linear mean gradient models. This hypothesis, probably attributable to de St. Venant or to Boussinesq, has appeared in different forms - usually incorporating an ad hoc estimate of the proportionality coefficient, the "eddy viscosity" or "eddy diffusivity" (for example, (1,2)).

In spite of the enormous development in turbulence modeling witnessed over the last two decades, the simplicity of the gradient transport models (GTM) - often with enough adjustable parameters - appears to be responsible for their persistent use in some areas of engineering practice, especially in meterology and oceanography. Among other things, gradient transport models require that the characteristic scale of the turbulent transporting mechanism must be small compared with the dimension characteristic of the inhomogeneity of the mean transported quantity. It has been pointed out many times (3-5) that nearly all turbulent flows violate this basic *a priori* requirement, and yet a reasonable degree of success has been claimed for the gradient transport models, especially in free shear flows. Therefore, a study directed towards determining the reasons for this (apparent) success of the GTMs appeared to be worthwhile; this is one of the goals of the present study.

Several instances can now be quoted which, over the years, have demonstrated the inadequacies of the GTMs (6-15). Mindful of these inadequacies to turbulence, several formal generalizations have been proposed (5, 16-18). Alternatively, it has been thought that formal generalizations do not address themselves to the heart of the problem, and so some *ad hoc* 'corrections' - which could even be drastic - have also been proposed, for example (19). However, the validity of any of these models in more than one situation remains to be tested. This is the second purpose of the present study. For this purpose, we designed several simple experimental configurations in some of which simple gradient transport models worked well but in some of the others did not. Presentation of the experimental data in these flows - with a possible relevance to turbulence modeling and the computation of complex turbulent flows forms yet another purpose of our paper.

FLOW CONFIGURATION

Figure 1 shows a schematic representation of the experimental configurations used here. The wind tunnel was of the open-return type with a nominal test section 30 cm x 30 cm, and about 3.65 m long. Air

flow was created by two axial fans in tandem. An essentially constant pressure field was created by adjusting the vertical walls.

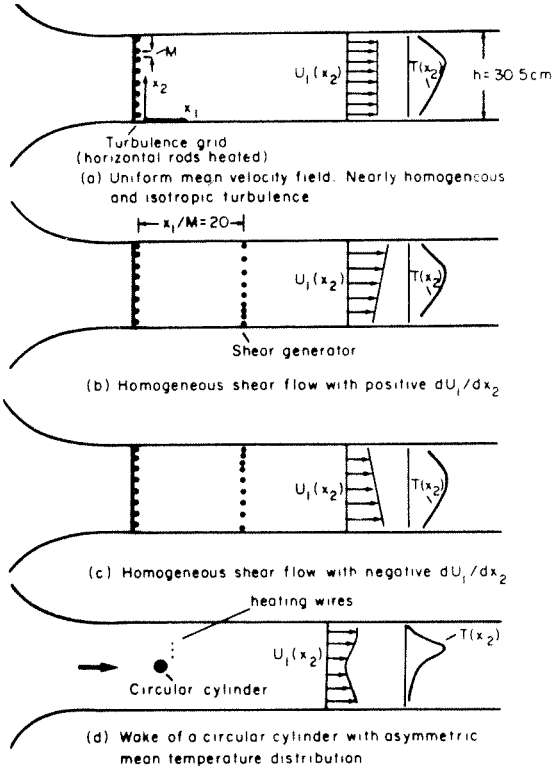

Fig. 1. Schematic of experimental set-up

Three homogeneous flows and one inhomogeneous shear flow were studied. One of the homogeneous flows was the uniform flow produced behind a square-mesh biplane cylindrical-rod grid with 2.54 cm mesh and solidity 0.36. The mean volocity was nominally uniform across the test section. The temperature field was created by electrically heating each of the horizontal rods of the grid separately, so that the desired inhomogeneous mean temperature field could be created (Figure 1a).

The two other homogeneous flows with nominally uniform positive or negative mean velocity gradient were created by placing a shear generator 20 mesh sizes downstream of the turbulence-generating grid (see Figures 1b and 1c). The shear generator is an array of horizontal non-uniformly spaced cylindrical rods (20) and could be inserted in the tunnel such that dU_1/dx_2 could be positive (Figure 1b) or negative (Figure 1c). The temperature field was created exactly as in the uniform flow case.

Lastly, the inhomogeneous shear flow studied here is the wake of a circular cylinder (d = 1.1 cm) in which the temperature field was produced by heating three thin parallel wires (diameter 0.127 mm) mounted asymmetrically with respect to the cylinder on a wooden frame which could be inserted (see Figure 1d) at any of the three locations (x_1/d = 1.2, 2.3, and 46) downstream of the cylinder. Also, the spacing between the wires, their transverse location with respect to the cylinder and the heating current in each of the wires could be adjusted independently to obtain within limits any desired mean temperature distribution.

INSTRUMENTATION

Mean velocity U_{10} along the tunnel centerline was measured with a pitot-static tube. The mean velocity profile $U_1(x_2)$ and the velocity fluctuations u_1 and u_2 were measured with a DISA 55P51 gold-plated X-wire probe, with sensing elements 5 μm in diameter and 1.25 mm in length, powered by two DISA 55D01 constant temperature anemometers; D.C. power supplies were used to minimize the noise level. The mean temperature profile $T(x_2)$ and the reference temperature upstream of the grid were measured with two Fenwall Electronics GC32M21 thermistor probes. The temperature fluctuation θ was measured with a DISA 55P31 platinum wire probe with the wire length of 0.4 mm and diameter 1 μm. The temperature wire was positioned vertically at a distance of about 0.5 mm from the nearest wire of the X-wire probe, and was operated at a constant current of 0.3 mA on a home-made constant current source (21). The operating current was low enough to render the velocity sensitivity of the temperature wire negligible. The temperature contamination of the velocity signals was eliminated by correcting them with the instantaneous local temperature measured with the temperature wire (22). The vertical position of the probes was adjusted with a variable speed motor and a gear mechanism.

All signals were amplified and low-pass filtered at an upper cut-off frequency of 5 kHz. The signals were also corrected for noise assuming that the noise was statistically independent of the signal. The signals were digitized and processed on a DEC PDP 11/40 digital computer.

RESULTS IN HOMOGENEOUS FLOWS

Mean Velocity and Mean Temperature Distributions

Measurements were made at x_1/M = 60 and 128 but, in most cases, only those made at x_1/M = 60 are reported here. In all the cases, there was a significant region of two-dimensionality in the mean quantities.

Figure 2 shows the distribution of mean velocity and mean temperature rise for the three homogeneous flows. For the uniform flow experiment, the mean velocity was uniform across the test section to within about 2% of the centerline velocity of 17.2 m sec^{-1}. The grid mesh Reynolds number was about 29100. The two other flows had roughly linearly varying mean velocity profiles (except for the last point in each case on the low velocity side). The centerline velocity U_{10} in both cases was 16.0 m sec^{-1}, and $|dU_1/dx_2|$ was 17.9 m sec^{-1}.

In all three cases, the mean temperature distributions were quite similar. The maximum mean temperature rise of 2.7°C was low enough to consider heat as a passive scalar. This was also verified by noting that the measured root-mean-square velocity intensities with and without heating were essentially the same. A measure of the inhomogeneity of the temperature field is given by the parameter $(dT/dx_2)\, L_g/T_{max}$. In the present experiments, this parameter was estimated to be as high as 0.5, signifying a sizeable inhomogeneity.

Root-Mean-Square Intensities

Figure 3 shows the transverse distribution of the normalized root-mean-square velocity fluctuations in the central two-thirds of the tunnel height. For the uniform grid flow, both u_1' and u_2' are uniform

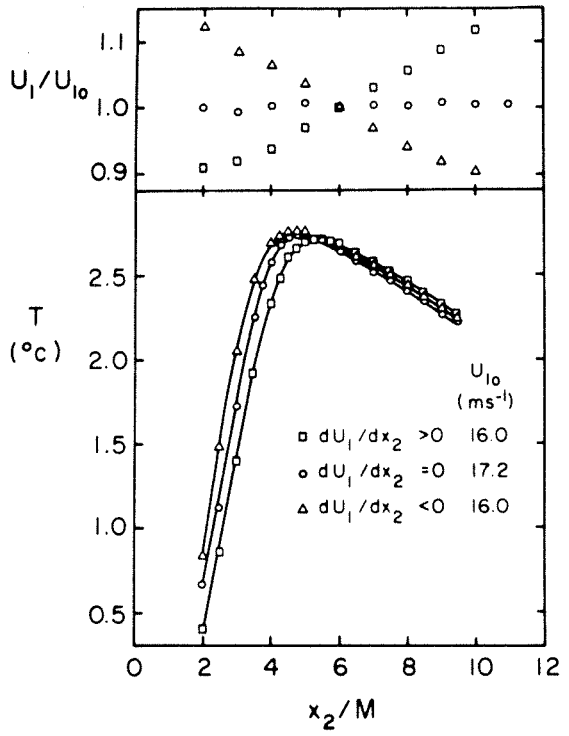

Fig. 2. Transverse distributions of mean velocity and mean temperature rise

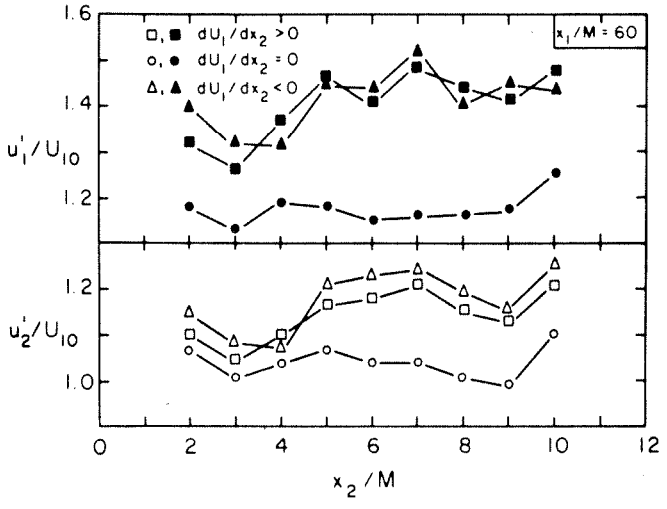

Fig. 3. Transverse variation of turbulence intensities

to within ±5%. The ratio $u_1'/u_2' \simeq 1.15$, quite comparable to that in other similar flows (23). For the shear flows, on the other hand, there is a ±12% variation in u_1'/U_{10} and about ±8% variation in u_2'/U_{10}. For the present purposes, these distributions are considered sufficiently homogeneous in the transverse direction. On the average, $u_1'/u_2' \simeq 1.23$. At $x_1/M = 128$, the turbulence intensity distributions are homogeneous to a somewhat better accuracy. Figure 4 shows the transverse distribution of the normalized root-mean-square temperature fluctuation.

Heat Transport in the x_2-Direction

Figure 5 is a plot of $\overline{u_2\theta}$ against the corresponding local values of dT/dx_2. Data are presented

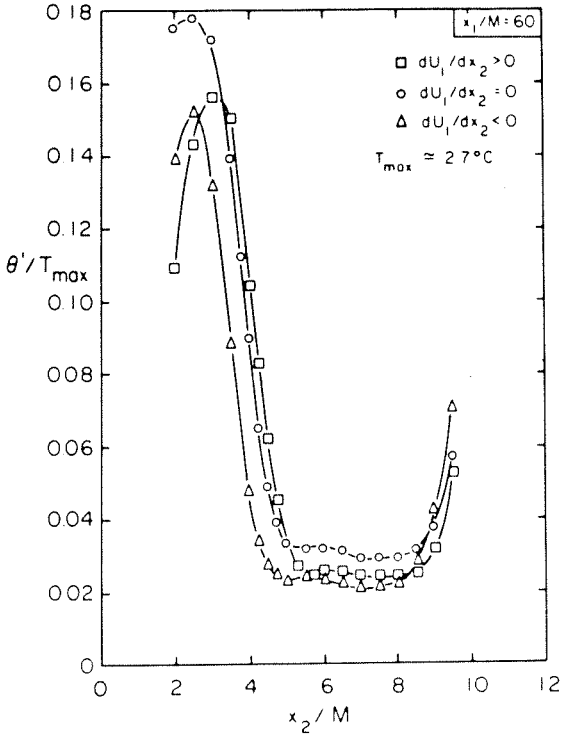

Fig. 4. Transverse variation of the root-mean-square temperature fluctuation

for x_1/M=60 and 128. A 6th order polynomial was fitted to the measured mean temperature distribution to obtain dT/dx_2. The estimated error bounds for both quantities are shown in the figure. It is clear that in all three cases $\overline{u_2\theta}$ is zero when dT/dx_2 is zero, and a gradient transport model with constant diffusivity is quite satisfactory.

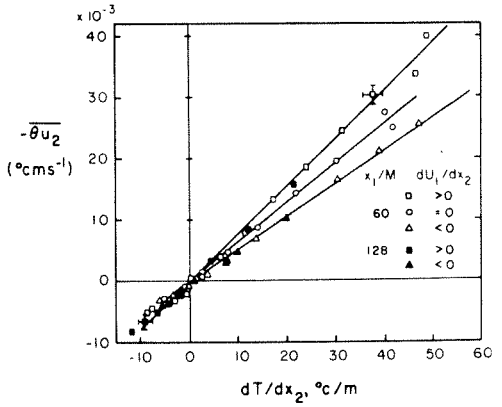

Fig. 5. Variation of heat flux with mean temperature gradient for the homogeneous flows

ASYMMETRICALLY HEATED WAKE

Measurements were made for several configurations of the heating wires and the wake generator, but results are presented here only for that shown in Figure 6. Measurements were made only at one station ($x_1/d \simeq 100$). It would have been desirable to have

made the measurements further downstream (where the flow would be self-preserving to a better degree of approximation), but the limitations of accuracy in heat transport measurements for small T led to this choice. Figure 6 shows transverse profiles of normalized velocity defect w/w_o (w_o = 1.78 ms^{-1}), u_2'/w_o, T, θ'/T_{max} and L_f/d; here L_f was obtained by evaluating the area up to the first crossing under the autocorrelation function of u_1 (24) and converting the resulting integral time scale to a length scale via Taylor's "frozen field" approximation. It is seen that even at $x_1/d \simeq 100$, the presence of the wires in the wake results in a slight asymmetry in the velocity near the maximum defect region, and stronger asymmetries in u_2' and L_f profiles.

Figure 7a shows a plot of the heat flux $-\overline{u_2\theta}$ and the mean temperature gradient $\partial T/\partial x_2$ at several points across the wake. Clearly, there is a small but finite region (the shaded region in the figure) in which the heat flux and the mean temperature gradient are of opposite sign implying negative diffusivity, or heat transport against the mean temperature gradient.

A more direct demonstration of the inadequacy of the GTMs is given in Figure 7b which shows that $-\overline{u_2\theta}$ when plotted against $\partial T/\partial x_2$ forms a closed loop. (If a GTM were applicable the loop would collapse on to a single curve through the origin; if the diffusivity were also constant, the curve would be a straight line.) For the discussion to follow, the rough correspondence between the various key points of this loop and their physical location is indicated by the use of the same letters A,B,C,D and E in Figures 7a,b and the inset to Figure 7b. Large negative x_2/d (say, around A in the inset) correspond to the vicinity of the origin in Figure 7b. As x_2/d increases (algebraically), both $\partial T/\partial x_2$ and $-\overline{u_2\theta}$ increase until at B the (positive) maximum value of $\partial T/\partial x_2$ is reached. Beyond B, $\partial T/\partial x_2$ decreases but $-\overline{u_2\theta}$ does not keep pace with $\partial T/\partial x_2$ and is finite and large even in the vicinity of C where $\partial T/\partial x_2$ is small. For even larger x_2/d, $\partial T/\partial x_2$ is negative (path CD) until the negative maximum of the temperature gradient is attained at D; around D, $-\overline{u_2\theta}$ is still decreasing (see Figure 7a), however. The path DE constitutes the return to $\partial T/\partial x_2 = 0$ as x_2/d approaches large positive values.

Corresponding regions in which the turbulent momentum transport $-\overline{u_1u_2}$ occurs against the direction of mean velocity gradient have been observed in many different flow situations (6-16). These regions have been called regions of "energy reversal" (9) or, more commonly in the later literature, as regions of "negative production", although the appropriateness of either term has been questioned. For example, it has been pointed out (25) that the total production terms are given by $-\overline{u_iu_j}\,\partial U_i/\partial x_j$, and that in the regions where $-\overline{u_1u_2}$ $(\partial U_1/\partial x_2)$ is negative, the other production terms $-(\overline{u_1^2}-\overline{u_2^2})\,\partial U_1/\partial x_1 - \overline{u_1u_2}\,\partial U_2/\partial x_1$ are positive and (though small) of the right magnitude to counteract locally the negative values of $-\overline{u_1u_2}\,\partial U_1/\partial x_2$. However, this conclusion is negated by other measurements (10,26) in which all the production terms except $-\overline{u_1u_2}$ $(\partial U_2/\partial x_1)$ were measured. In these two latter cases, the magnitude of the negative values of the total production is very small indeed. Lastly, we may mention Hinze's (16) conclusion that even if the sum-total of production terms is negative, it does *not* imply energy transfer back to the mean flow.

In the heat transfer case, there are fewer measurements of the $\overline{\theta^2}$-production terms (14,19,27), but the balance of evidence does suggest that the total thermal production terms

$$-\overline{u_2\theta}\,\partial T/\partial x_2 + \overline{u_1\theta}\,\partial T/\partial x_1$$

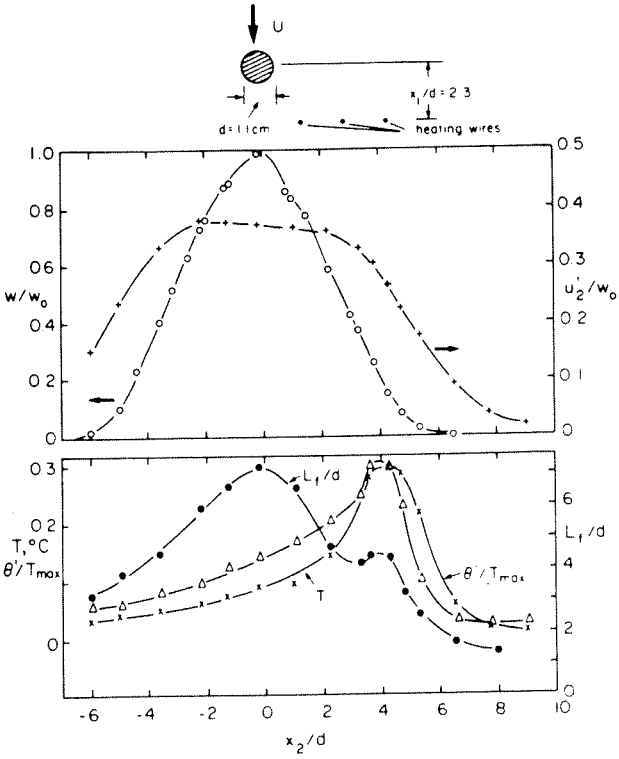

Fig. 6. A representative cylinder/heating wire combination and the resulting transverse distributions of mean defect velocity and temperature rise

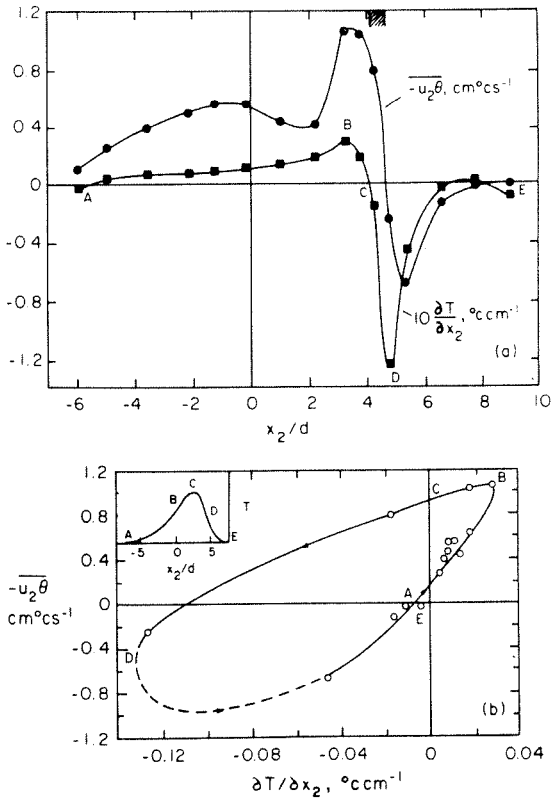

Fig. 7. Variation of heat flux with mean temperature gradient for the asymmetrically heated wake

add up to negative values in some small flow region. In the present wake, mean temperature profiles were not measured sufficiently closely to evaluate $\partial T/\partial x_1$ accurately, but rough estimates suggest that the inclusion of $-\overline{u_1\theta}\ \partial T/\partial x_1$ does not alter the sign of total production in any substantial way.

TEST OF GENERALIZED MODELS

For lack of space, we shall restrict to testing the performance of these models without discussing the basis of their formulation. Specifically, we consider the following models which, in order, are the GTM and models due to Corrsin (5), Lumley (17) Kronenburg (18), Beguier-Fulachier-Keffer (19) - BFK for short-and Townsend (28):

$$-\overline{u_2\theta} = D\,(\partial T/\partial x_2) \equiv R_G \qquad (a)$$

$$-\overline{u_2\theta} = D\,(\partial T/\partial x_2) + L_f T\,(\partial u_2'/\partial x_2) \equiv R_c \qquad (b)$$

$$-\overline{u_2\theta} = D\,(\partial T/\partial x_2) + (T/2)\,(\partial D/\partial x_2) \equiv R_L \qquad (c)$$

$$-\overline{u_2\theta} = D\,(\partial T/\partial x_2) + L_f\,\partial/\partial x_2\,(D\,\partial T/\partial x_2) \equiv R_K \qquad (d)$$

$$-\overline{u_2\theta} = D\,(\partial T/\partial x_2) + K_\theta\,\ell_\theta^3(\partial q'/\partial x_2)\,(\partial^2 T/\partial x_2^2) \equiv R_B \qquad (e)$$

$$-\overline{u_2\theta} = D\,(\partial T/\partial x_2) - V_c\,T_{max} \equiv R_T \qquad (f)$$

All models have been considered to the first order of correction. For convenience in evaluation, we have here replaced D by $L_f\,u_2'$; a more appropriate definition would presumably differ from the present one by a constant factor that is immaterial in the present context.

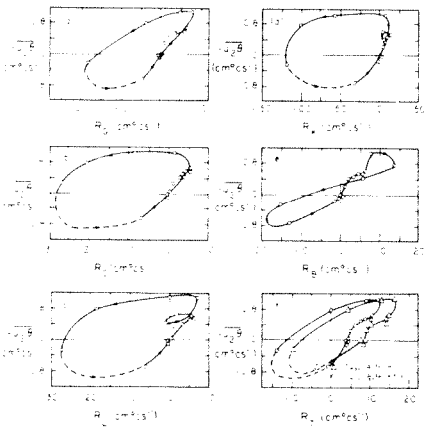

Fig. 8. Test of generalizations of GTM for the present asymmetrically heated wake

Any improved alternative to the GTM must be capable of collapsing the closed loop in Figure 7b on to a single curve or nearly so. From both Figures 8 and 9, the models due to Corrsin (5) and Lumley (17) appear to aggravate rather than improve the situation. The Kronenburg model appears to work reasonably well for the mixing layer data (19), but has poor performance in the present flow. For testing model (e) using the present flow data, we have replaced q' by $\sqrt{3/2(\overline{u_1^2} + \overline{u_2^2})}$. This introduces an uncertainty in the precise value of K_θ, which should be -0.11 according to (19). Several values in the vicinity of -0.11 were tried, but the performance of the model was worse than that of GTM for all negative K_θ. There is no physical or mathematical reason why K_θ must be only negative, and so we tried positive values as well. Figure 8e shows that for $K_\theta = 0.015$, the model performs reasonably well. However, the significance of a model with a coefficient whose sign itself is uncertain is not clear. In Townsend's model, the correction due to the bulk transport is a constant number on the right hand side, and this can only translate the closed loop without either shrinking or enlarging it. The effect is shown in Figure 8f for two values of the correction, and in Figure 9f for one.

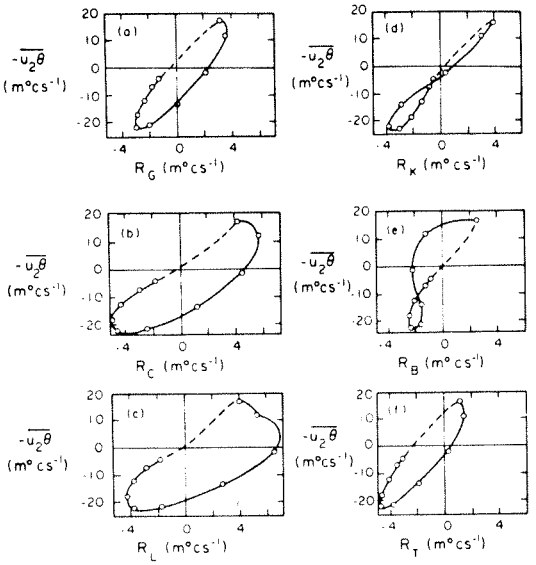

Fig. 9. Test of generalizations of GTM for the asymmetrically heated mixing layer (19)

DISCUSSION

Our experiments have emphasized that the GTM which appears perfectly adequate with a constant diffusivity for the homogeneous flows cannot handle inhomogeneous flows even qualitatively. The chief difference between the homogeneous and inhomogeneous shear flows is the dominance of the large structure in the latter; it appears that the large structures are responsible for a sizeable fraction of the transport process, and it is in the modeling of these effects that none of the generalizations of the GTM discussed earlier has had reliable success. One of the currently held views is that a turbulent shear

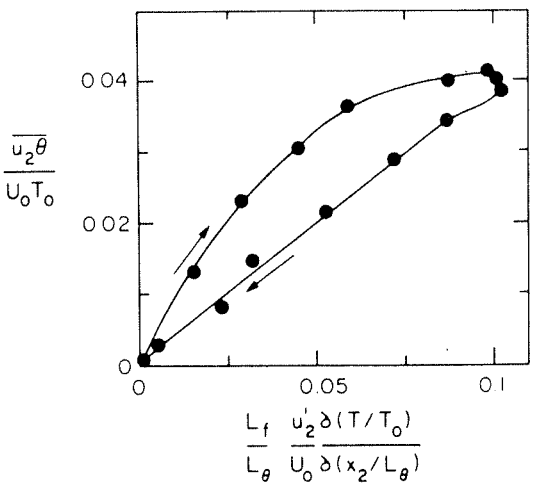

Fig. 10. Variation of heat flux with mean temperature gradient in a symmetrically heated co-flowing jet (29)

flow is essentially a consequence (and not the cause) of these transport-efficient large structures and their mutual interactions. If this view is correct, an altogetherly different approach, which does not even invoke a mean field, is necessary before the problem can be resolved.

Finally, we examine briefly the reason that the GTM seems to work well in free shear flows. Figure 10 shows a plot of $u_2\theta$ vs $(\partial T/\partial x_2)$- now appropriately normalized - for one half of a symmetrically heated co-flowing jet (29). It is again seen that the data form a loop instead of a single curve. However, the flow symmetry about the centerline forces both $u_2\theta$ and $\partial T/\partial x_2$ to be zero at the same point, so that the return part of the loop is now constrained to go through the origin. This results in a much smaller loop than would be the case if asymmetries existed. This is the reason for the apparent success of the GTM in symmetric flows.

ACKNOWLEDGMENT

This research was supported by the Atmospheric Science Division of the National Science Foundation.

REFERENCES

1 Monin, A.S. and Yaglom, A.M. "Statistical Fluid Mechanics: Mechanics of Turbulence," Vol. 1, 1971, M.I.T. Press, Cambridge (Ed. J.L. Lumley).

2 Hinze, J.O., "Turbulence," 1976, McGraw Hill Co., New York (Second Edition).

3 Batchelor, G.K., "Note on Free Turbulent Flows, with Special Reference to the Two-Dimensional Wake," Journal of Aeronautical Sciences, Vol. 17, 1950, pp. 441-445.

4 Corrsin, S., "Heat Transfer in Isotropic Turbulence," Journal of Applied Physics, Vol. 23, 1952, pp. 113-118.

5 Corrsin, S., "Limitations of Gradient Transport Models in Random Walks and in Turbulence," Advances in Geophysics, Vol. 18A, 1974, pp. 25-60.

6 Eskinazi, S. and Yeh, H. "An Investigation of Fully Developed Turbulent Flows in a Curved Channel," Journal of Aeronautical Sciences, Vol. 23, 1956, pp. 23-31.

7 Mathieu, J. and Tailland, A., "Étude d'un Jet Plan Dirigé Tangentiellement à une paroi," C.R. Academy of Sciences, Vol. 256, 1963 pp. 2768-2771.

8 Gee, M.T., and Bradshaw, P. "Turbulent Wall Jets with and without External Stream," NPL 3252 June 1960, Aeronautical Research Council, England.

9 Eskinazi, S. and Erian, E.F. "Energy Reversal in Turbulent Flows," Physics of Fluids, Vol. 12, 1969, pp. 1988-1998.

10 Erian, E.F., "Influence of Pressure Gradient on Turbulent Flow with Asymmetric Mean Velocity," ASME-Journal of Applied Mechanics, Vol. 91, 1969, pp. 901-904.

11 Hanjalic, K. and Launder, B.E., "Fully Developed Asymmetric Flow in a Plane Channel," Journal of Fluid Mechanics, Vol. 51, 1972, pp. 301-335.

12 Palmer, M.D. and Keffer, J.F., "An Experimental Investigation of an Asymmetrical Turbulent Wake," Journal of Fluid Mechanics, Vol. 53, 1972, pp. 593-610.

13 Fabris, G., "Conditionally Sampled Turbulent Thermal and Velocity Fields in the Wake of a Warm Cylinder and its Interaction with an Equal Cool Wake," Ph.D. dissertation, Illinois Institute of Technology, 1979.

14 Charney, G., Schon, J.P., Alcaraz, E. and Mathieu, J., "Thermal Characteristics of a Turbulent Boundary Layer with Inversion of Wall Heat Flux," Proceedings of the Symposium on Turbulent Shear Flows, Penn. State University, University Park, 1977, pp. 15.47-15.55.

15 Morel, R., Awad, M. Schon, J.P. and Mathieu,J., "Experimental Study of an Asymmetric Thermal Wake," In Structure and Mechanism of Turbulence, Vol. 1 1978, pp. 36-35. Lecture Notes in Physics, Springer-Verlag, Berlin.

16 Hinze, J.O., "Turbulent Flow Regions with Shear Stress and Mean Volocity Gradient of Opposite Sign," Applied Science Research, Vol. 22, 1970, pp. 168-175.

17 Lumley, J.L., "Modeling Turbulent Flux of Passive Scaler Quantities in Inhomogeneous Flows," Physics of Fluids, Vol. 18, 1975, pp. 619-621.

18 Kronenburg, C., "On the Extension of Gradient -Type Transport to Turbulent Diffusion in Inhomogeneous Flows," Applied Science Research, Vol. 33, 1977, pp. 163-175.

19 Beguier, C., Fulachier, L. and Keffer, J.F., "The Turbulent Mixing Layer with an Asymmetrical Distribution of Temperature," Journal of Fluid Mechanics, Vol. 89, 1978, pp. 561-587.

20 Rose, W.G., "Results of an Attempt to Generate a Homogeneous Turbulent Shear Flow," Journal of Fluid Mechanics, Vol. 25, 1966, pp. 97-120.

21 Tavoularis, S., "A Circuit for the Measurement of Instantaneous Temperature in Heated Turbulent Flows," Journal of Physics, E: Scientific Instruments, Vol. 11, 1978, pp. 21-23.

22 Tavoularis, S. and Corrsin, S., "Experiments in Nearly Homogeneous Turbulent Shear Flow with a Uniform Mean Temperature Gradient. Part 1," Journal of Fluid Mechanics, Vol. 104, 1981, pp. 311-347.

23 Comte-Bellot, G. and Corrsin, S., "The Use of a Contraction to Improve the Isotropy of Grid-Generated Turbulence," Journal of Fluid Mechanics, Vol. 25, 1966, pp. 657-682.

24 Comte-Bellot, G. and Corrsin, S., "Simple Eulerian Time Correlation of Full and Narrow-Band Velocity Signals in Grid-Generated, 'Isotropic' Turbulence," Journal of Fluid Mechanics, Vol. 48, 1971, pp. 273-337.

25 Wilson, J.D., "Turbulent Transport of Mean Kinetic Energy in Countergradient Shear Stress Regions," Physics of Fluids, Vol. 17, 1974, pp. 674-675.

26 Beguier, C., "Mesures de Tensions de Reynolds dans un écoulement dissymetrique en régime turbulent incompressible," Journal de Mécanique, Vol. 4, 1965. pp. 319-334.

27 Fulachier, L., Keffer, J.F. and Beguier, C., "Production Negative de Fluctuations Turbulentes de Température dans le case d'un Créneau de Chaleur s'épanouissant dans une Zone de Mélange," C.R. Academy of Sciences, Vol. 280, Series B, 1975, pp.519-522.

28 Townsend, A.A., "The Structure of Turbulent Shear Flows," 1956, University Press, Cambridge, England.

29 Antonia, R.A., Prabhu, A. and Stephenson, S. E., "Conditionally Sampled Measurements in a Heated Turbulent Jet," Journal of Fluid Mechanics, Vol. 72, 1975, pp. 455-480.